

Investigation of Microstructure of the Weld Zone of Hastelloy X Via Pulsed Nd-YAG Laser Welds

F. Najafzadegan^{a,*}, H. Mansori^b, M. Shamanian^c

^a Department of Materials Engineering, Najafabad Branch, Islamic Azad University, Isfahan, Iran.

^b Department of Materials Engineering, Malek-E-Ashtar University, Isfahan, Iran.

^c Department of Materials Engineering, Isfahan University of Technology, Isfahan, Iran.

ARTICLE INFO

Article history:

Received 27 Aug 2013

Accepted 01 Dec 2013

Available online 25 Dec. 2013

Keywords:

Nd-YAG laser

Hastelloy X

Microstructure

ABSTRACT

In the present study, microstructure of the welded zone of Hastelloy X sheets with thickness of 1 mm via pulsed Nd-YAG laser welding was studied. This welding process was carried out by autogenous and conductive method. Microstructure was observed by metallurgical OM and SEM. Results showed that solidification of the weld metal is dendritic. The dendrites in the central zone of the welding are fine and equiaxed while they are larger and columnar in the fusion boundary. Epitaxial growth was observed in the interface of base metal and weld metal. Alloy elements segregation did not occur during the solidification process and fine cracks were not observed in the welding zone of the alloy. Micro hardness results indicated that the hardness of welded metal was more than base metal and caused the decrease of grain size in welded metal more than base metal. This phenomenon occurred due to more differences between heating and cooling rate in this welding process.

1. Introduction

Super alloys are alloys resistant to temperature, corrosion and oxidation and in terms of chemical composition consist of three groups: nickel based, nickel-iron based and cobalt based [1].

Nickel-based super alloys are widely used as turbine high temperature components due to their excellent resistance to creep, fatigue and corrosion [2].

Hastelloy X super alloy is a nickel based alloy strengthened by solid solution. This alloy is issued in rocket combustion chamber jet and or jet engines. The final heat treatment of this alloy includes solution annealing at 1175°C and then

rapid cooling in air to achieve appropriate structure [3]. Hastelloy X alloy is usually used in condition of solution annealing at 1175°C and is specifically designed for long-term services of 10,000 hours at temperatures up to 900° C. Alloying elements of this alloy are chosen in a way to increase the mechanical properties and improve the corrosion at high temperatures, creep resistance, fracture toughness, and structural stability [1, 4- 6].

Since the amount of the elements such as Al, Hf, Ta, and Ti is very low in Hastelloy X, γ' does not appear to be able to form in the structure of this alloy. Microstructure of the alloy is composed of an austenite matrix and

Corresponding author:

E-mail address: najafzadeh_f@yahoo.com (Farrokh Najafzadegan).

Table 1. Chemical composition of hastelloy x.

Element	Ni	Cu	Fe	Cr	Mo	Co	C	Si	Mn	Al	V	Nb	W
(wt.%)	40.05	0.08	21.43	24.79	10.56	0.58	0.02	0.33	0.61	0.19	0.08	0.1	0.68

Table 2. Laser welding parameters.

Power (kW)	Peak power per pulse (kW)	Pulse frequency (Hz)	Focused Beam diameter (mm)
2	6	1	1

M₆C carbide enriched in Mo element [8]. According to the measurements conducted by Lippold et al. in Hastelloy X super alloy, solidification is attributed to the formation of austenite phase while M₆C is present until the end of the solidification process [12]. Zhang Lee et al. have found that through autogenous welding of Hastelloy X to Mar-M 247 by CO₂ laser welding, the hardness and strength in the welding zone of the Hastelloy X is due to M₆C carbides and their distribution. The observations have shown that carbides' size in the weld metal is almost 0.2 μm and they are separately distributed in the microstructure which is among the advantages of rapid solidification through the laser welding process [9, 11]. Stoloff observed that precipitation of fine carbide particles in the matrix of Hastelloy X increased the strength of the alloy [16]. Within the melting welding, the metal-based particles in the fusion line serve as matrix for nucleation. Due to the fact that the melted metal in the weld pool is in direct contact with these matrix grains and completely wets these particles, crystals nucleation occurs from the melted metal and on these grains. The process is typically called epitaxial growth [15]. Zhang Lee et al. observed that during the CO₂ laser welding, Hastelloy X dissimilar with Mar-M247 alloy was formed through the epitaxial growth process in the interface of weld metal and base metal in the Hastelloy X [9].

Among welding methods that can be performed on this alloy, one can refer to arc welding with tungsten electrode, laser, and electron beam welding [7]. Laser welding has some advantages compared to other methods including high welding width to depth ratio, low heat input, high welding speed, small heat-affected zone and low distortion. Types of laser used in industry include CO₂ and Nd:YAG

lasers which are used as continuous and pulsed. Pulsed Nd:YAG laser is paid more attention due to higher penetration and lower power consumption [8]. The welding with pulsed Nd:YAG laser has allocated a smaller percentage of researches to itself compared to other techniques. In the present study, microstructure of the weld zone of Hastelloy X was studied. Welding is performed with the use of pulsed Nd:YAG laser and welding process is carried out as autogenous. Initially, the laser welding approximate parameters were determined by using the existing scientific experiences, and finally optimal parameters were determined to obtain a weld with full penetration depth and optimal mechanical properties. After welding, mechanical properties of weld zone (including weld metal, heat – affected zone) were discussed.

2. Experimental

Hastelloy X super alloy sheets with 1 mm thickness were used in this research. Sheet chemical analysis was performed by Belec device. Chemical composition of Hastelloy X is shown in Table 1. Welding was done by using pulsed Nd:YAG laser method and without using the filler metal. To determine the optimal parameters, welding operation was done with consideration of the scientific experiences about Hastelloy X alloy welding. At first, the junction of sheets was cleaned with fat removal by steam and ultrasonic. Welding operation was performed by using the optimal parameters (70watts of power, 5.03ms pulse width and welding speed of 8 mm per minute). Welding was done conductively and with the use of high purity argon shielding gas. Parameters used in laser welding are shown in Table 2. Microstructure was observed by metallurgical OM and SEM device (VEGA-TSCAN). To

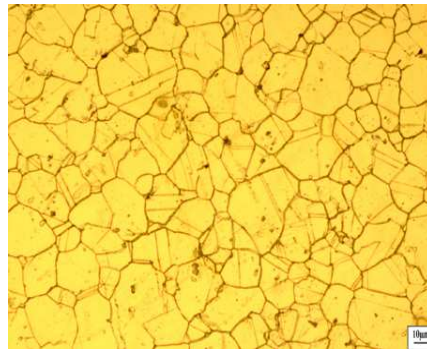
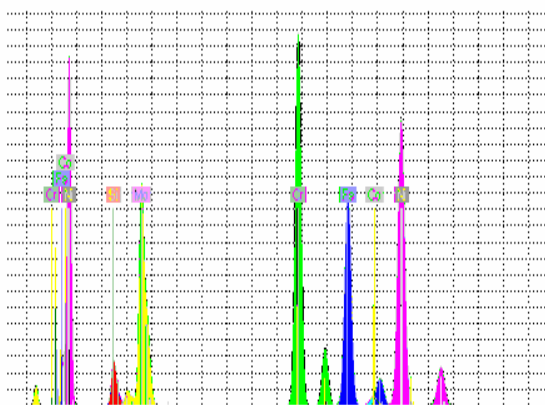


Fig. 1. Optical microscope image of Hastelloy X.



Element				
	Series	unn. C [wt.-%]	norm. C [wt.-%]	Atom. C [at.-%]
Silicon	K series	0.96	1.01	2.09
Chromium	K series	21.20	9.31	24.87
Iron	K series	18.09	19.04	19.76
Cobalt	K series	0.90	0.95	0.94
Nickel	K series	44.85	47.19	46.60
Molybdenum	L series	9.03	9.50	5.74
Total:		95.0 %		

Fig. 2. SEM/EDS spectrum from base metal

study the mechanical properties of samples, Micro-hardness measurement tests were carried out by AFFRI device (Italy, DM88). Micro-hardness measurement test was done on welded samples by Vickers method in accordance with standard ASTM E 384. The amount of applied load was selected 100 gr based on effect size amount and in accordance with standard ISO 6507-1. Hardness profile was done in a region with 2.5 mm length from both sides of weld central line with 50 effect points in the width of weld zone.

3. Results and Discussion

Investigated Hastelloy X is an alloy strengthened with solid solution which has become solution annealed at $t_{1175^{\circ}C}$. Chemical analysis of this alloy indicates the presence of a small amount of elements such as Al, Ti, Ta, and Hf in chemical composition. The conditions for γ' precipitated formation in the microstructure of this alloy aren't present due to the small amount of Al and Ti.

Optical microscopy image of Hastelloy X microstructure is given in Fig1. The microstructure of this alloy includes continuous phase γ in the context along with anneals twins. Grain size in base metal was determined $40.5\mu m$ by image analysis software.

Electron microscopy image of existing particles in Hastelloy X alloy context is shown. The microstructure of this alloy includes high percentage of solid solution elements (Co,Fe,Cr,Mo,W) in the context.

EDX spectroscopy was performed for existing particles and the results are given in Fig 2. There is a significant difference between weight percentage of nickel and other elements. The microstructure of this alloy includes fine particles that are distributed in the context as shown in Fig 1.

Electron microscopy image of the existing particles in Hastelloy X alloy context shows that particles existing in the context are M_6C carbides enriched by molybdenum. J.C.Lippold, H.Tawancy et al. also observed these carbides

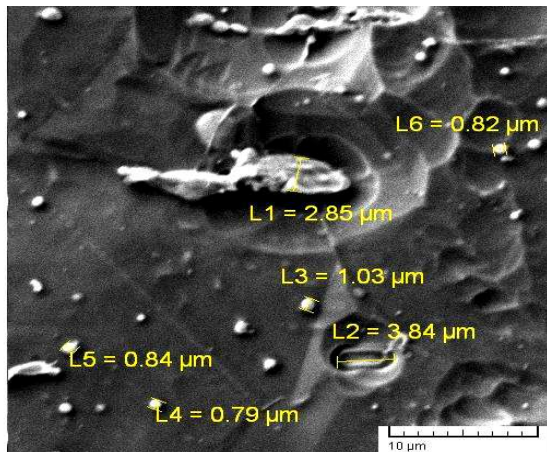


Fig. 3. SEM microstructure of carbides in base metal.

in the context [8, 12]. The size and distribution of carbides has a direct strength. The size of carbides in base metal was measured to compare the size of carbides in weld metal. Average size of carbides in base metal is $1.695\mu\text{m}$ (Fig 3).

Grain size investigation in weld metal compared to grain size in base metal has special importance to evaluate the mechanical properties of weld metal and base metal. Grain size has a direct effect on mechanical and strength properties of weld zone. The observations of Mat O. et al. and Zhang Lee indicate that the structure of weld metal in the laser welding process involves finer grains with higher hardness as compared to the GTAW welding [9].

Two areas of base metal and weld metal are seen in Fig 4. Microstructure of weld metal includes fine grains in welding with laser method. Grain size in weld metal and in base metal was determined by image analysis software as $2.33\mu\text{m}$ and $40.5\mu\text{m}$, respectively. Significant difference between grain size in base metal and weld metal is due to the high speed of heating and cooling in laser welding. The smaller grain size of weld metal compared to that of the base metal has resulted in more hardness of the weld metal compared to the base metal. Electron microscopy image of carbides existing in the weld metal shows that carbides are distributed uniformly in the entire weld zone. Besides, the particles distributed between the intra-dendritic are M_6C carbides.

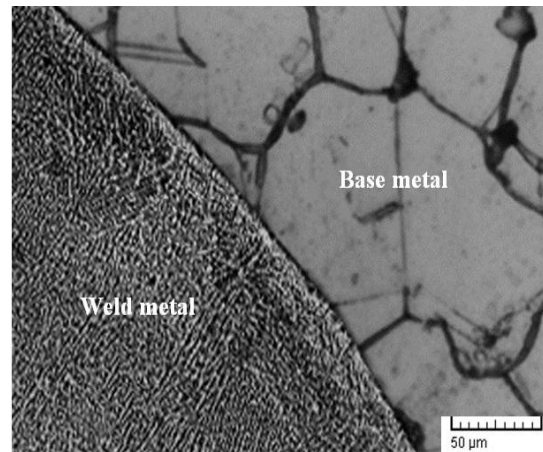


Fig. 4. SEM microstructure of base metal, weld metal, joint region.

Average size of carbides in base metal is $1.695\mu\text{m}$ that reaches to $0.25\mu\text{m}$ in weld metal, as can be seen in Fig 5. This comparison shows that carbides in weld metal are much smaller than carbides in base metal. Zhang Lee et al. also found the results similar to the present study and also observed that molybdenum-rich M_6C carbides in the microstructure determined the size of carbides in weld metal as $0.2\mu\text{m}$ [9]. During the Hastelloy X welding, without using the filler metal, the melted metallic atoms are displaced and then located on the matrix particles and nucleate without any change in the crystallographic positions. Such a process is known as epitaxial growth. During this growth, the main body of the columnar dendrites grows in particular directions [15]. Besides, all dendrites growing from the same particle are placed in the same orientation where this orientation is different from one particle to the adjacent ones. As shown in Fig 6, because of the epitaxial growth of the grains boundary, these boundaries in the heated zone are bound to the welding zone. As it was previously mentioned, Zhang Lee et al. observed Hastelloy X dissimilar with Mar-M247 alloy formed within the epitaxial growth process in the interface of weld metal and base metal in the Hastelloy X [9]. Solidification in the Hastelloy X occurs in the dendritic form. The rapid solidification of the weld metal, which is among the intrinsic traits of the laser welding, leads to formation of a very fine dendritic structure in the welding zone. Specifically, the laser welding reveals

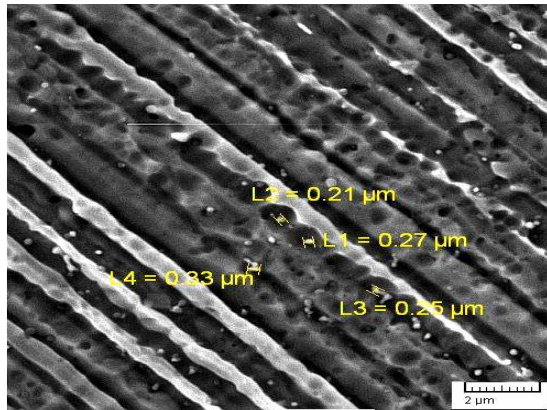


Fig. 5. SEM microstructure of carbides in weld metal.

narrow heat-affected zones induced by the very low and concentrated heat input. Metallurgical properties of the laser welding bounds are determined by the microstructure produced from rapid solidification, whereas the microstructure obtained from the solidification is in turn controlled by solidification conditions (solidification rate (R), thermal gradient (G)). Solidification rate has the minimum and maximum values in the central zones of the welding and fusion line, respectively. The thermal gradient in the direction perpendicular to the weld pool boundary reaches to its minimum and maximum values in the central zone of the melting and in fusion line, respectively. Besides, when moving from the fusion line to the inside of the welding zone, thermal gradient reduces. Formation of the structure with equiaxed dendrites within the welding and relatively thick columnar dendrites in the areas near to the fusion line can be explained based on thermal gradient (G), cooling rate, and growth rate (R). Moreover, G/R ratio is the critical controlling parameter which governs microstructure of the solidification. When moving from the fusion line towards its central part, G/R ratio decreases. Therefore, it can be predicted that throughout the melting zone, solidification changes from planar to cellular, columnar dendritic, and equiaxed dendritic. According to Fig 7, once G/R ratio is large enough, solidification process produces columnar dendritic structure. In other words, formation of the columnar dendritic structure near to the fusion line is due to the decreased growth rate

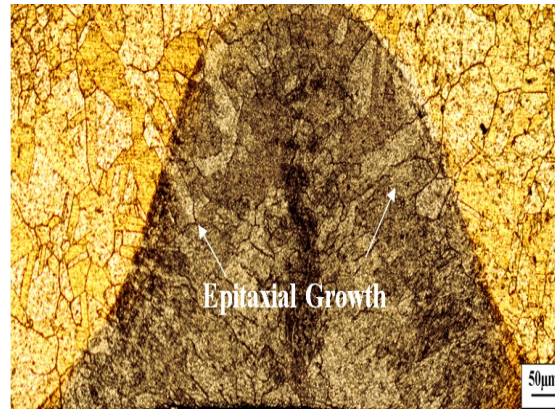


Fig. 6. Microstructure of Epitaxial Growth the fusion boundary.

and increased thermal gradient in the fusion line. Thermal gradient in the weld pool near to the weld boundary is more severe than that of its central parts and a decreased G/R ratio leads to formation of fine equiaxed dendrites near the central parts of the welding (Fig 8). Dendrites are fine and equiaxed in the central parts of the welding, while they are coarser and columnar in the vicinity of the welding zone. These morphological differences can be observed with higher resolution using greater magnifications. Ming Pang et al. also observed the finding similar to those of our work and reported that once G/R ratio is relatively low, solidification process tends to form equiaxed dendritic structure [13]. In the central part of the welding, equiaxed dendrites nucleate and grow and, thus, prevent formation of columnar dendrites. Thermal gradient decreases when moving from welding zone toward its central parts. So, one can conclude that a significant reduction in thermal gradient in the conventional direction (from fusion line to its central zone) leads to formation of equiaxed microstructure. In the central zones, growth direction is not uniform and the produced microstructures with dendritic structure do not show a preferred orientation as they grow. Janak Ram et al. also reported results similar to those of the present work. Also, in the microstructure of the central part of the Hastelloy X welding, not only the equiaxed grains are observed, but also the growth of the dendritic structure is not performed in a particular direction (fig 9).

Segregation is a time dependent process and

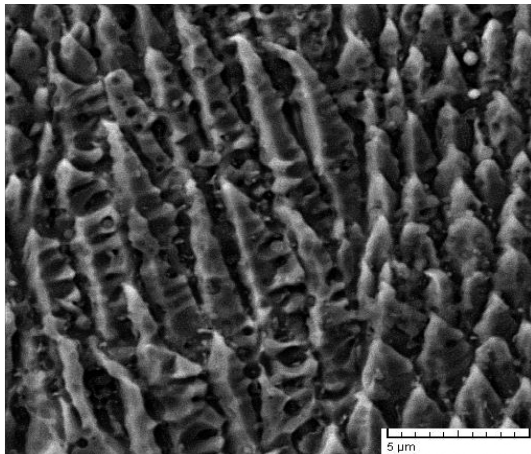


Fig. 7. Fusion zone microstructures showing columnar dendrites adjacent to the fusion boundary.

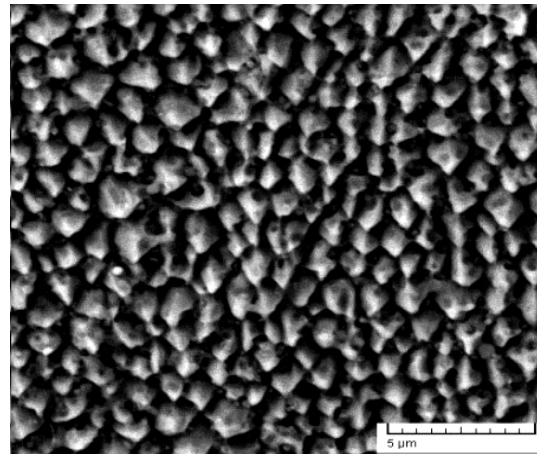


Fig. 8. SEM microstructure showing very fine equiaxed dendrites in the weld interior.

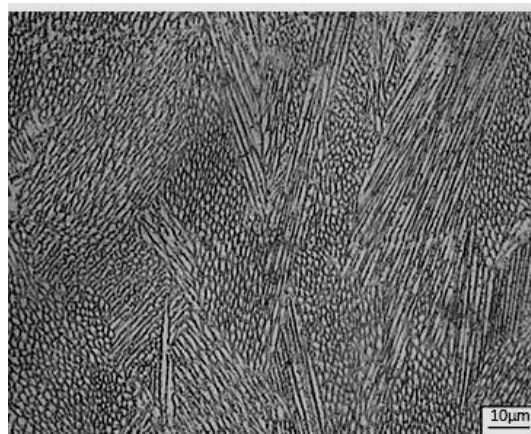
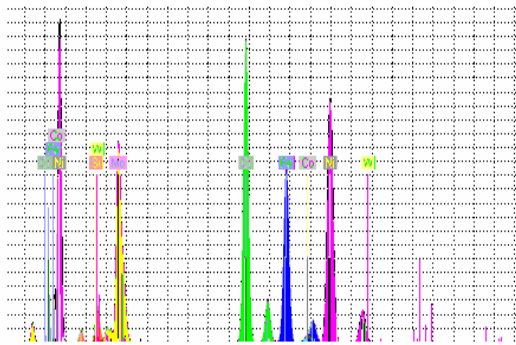


Fig. 9. Formation fine equiaxed grain in the weld interior.

then is affected by the solidification rate of the weld, as well as various factors such as heat input, welding process, etc. During the solidification process, segregation occurs because of the formation of a liquid enriched with elements and depletion of some other elements. According to Zhang Lee et al., fine cracks develop in the welding zone of Hastelloy X when the alloy elements are dilute enough and the phase strength reduces [9]. Zhang Lee et al. did not observe fine cracks in the welding zone of the Hastelloy X welded by CO₂ welding [9]. These cracks also were not observed in the present work when applying Nd:YAG laser. To evaluate possibility of the segregation from intra-dendritic spaces, EDS spectroscopy was performed. After the examinations it was found that the intra-dendritic space is rich in Cr, Ni, Fe, and Mo. The results of spectroscopy

of the intra-dendritic space are shown in Fig 10. A comparison between EDS spectroscopy results of the base metal and intra-dendritic space indicated that the chemical composition of the elements in the intra-dendritic space is similar to that of the base metal. Moreover, a comparison between the EDS spectroscopy results of the intra-dendritic space with EDS spectroscopy results of the base metal illustrates that segregation does not occur during the solidification process of the Hastelloy X super alloy; hence, phase strengths do not decrease. This is why cracks were not observed in the welding zone of the Hastelloy X using the laser welding in the present work. The low cooling rate results in the large dendrites arm spacing as compared to the rapid cooling rate. These coarse spaces are preferred sites for segregation of the alloy elements during the solidification. It means that in case the cooling rate is slow, intra-dendritic phase can be formed more conveniently. To improve properties of the welding, it is required to decrease segregation process by controlling the cooling rate/ heat input by applying appropriate welding methods. The heat input and welding rate can affect the distances among the dendrites arm spacing and the distance between the cells. The gradual cooling rate leads to the large dendrites arm spacing as compared to the rapid solidification welding. An increase in heat input (Q) and welding velocity (V) results in the increase of cooling rate, which in turn, A decreases the dendrites arm spacing. The mean distance dendrites arm spacing



Element	Series	unn. C [wt.-%]	norm. C [wt.-%]	Atom. C [at.-%]
Silicon	K series	0.15	0.15	0.32
Chromium	K series	20.80	21.60	24.36
Iron	K series	18.44	19.15	20.11
Cobalt	K series	0.95	0.99	0.98
Nickel	K series	46.40	48.18	48.15
Molybdenum	L series	9.55	9.91	6.06
Tungsten	L series	0.01	0.01	0.00

Fig. 10. SEM/EDS spectrum from interdendritic regions.

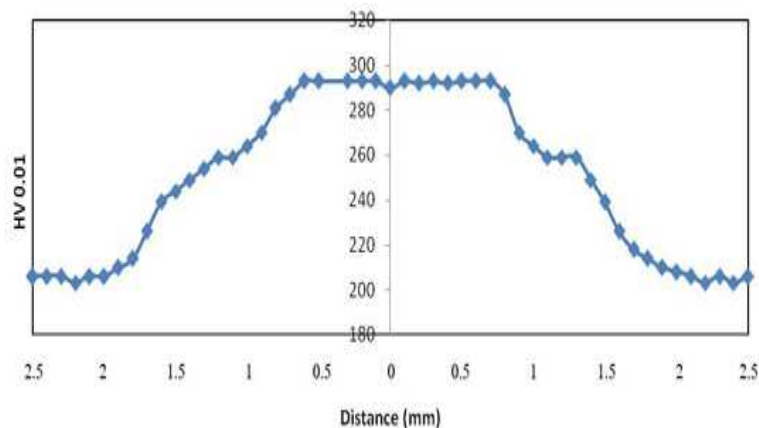


Fig. 11. Graph of the micro hardness measuring test of Hastelloy X.

is estimated as $0.38 \mu\text{m}$. A decrease in the ratio between input heat and welding rate (Q/V) leads to the increased cooling rate; which in turn results in decrease of the dendrites arm spacing. Since these spaces are the preferred spots for segregation of the alloy elements during the welding solidification process, they are very important. In comparison to GTAW method, during laser welding, the dendrites arm spacing decreases Q/V ratio. The number of preferred sites for alloy element segregation decreases during solidification and then segregation process does not occur.

Micro-hardness measurement test was conducted on the samples to investigate the mechanical properties of base metal, weld metal and heat affected zone of Hastelloy X alloy. The results of micro-hardness test are given in Table 3. The graph of micro hardness measurement test (hardness value in terms of distance from the weld central line) is shown in Fig 11. Hardness curve is symmetrical on both sides of the weld central area. Base metal

hardness was measured 211 ± 5 Vickers. The hardness value has increased with a specific slope from heat affected zone, on approaching the weld zone until it has become constant in the weld zone and become repeatable in number 295 ± 5 as shown in Table 3. Weld metal hardness is more than base metal hardness to the amount of 84 Vickers; it can be resulted from the decrease in grain size and the decrease in carbides size and distribution in weld metal compared to base metal, a phenomenon which is caused by high speed heating and cooling in laser welding.

4. Conclusions

Grain size in weld metal of the Hastelloy X and base metal was determined as $2.33 \mu\text{m}$ and $40.5 \mu\text{m}$, respectively. The significant difference in grain size of the weld metal as compared to the base metal is attributed to the high cooling rate of the welding during laser welding. The carbides observed in the base metals and weld metal are rich in molybdenum (M_6C). Carbides

Table 3. Results of microhardness measurements.

Hardness (Hv)	Region
295±5	Weld metal
211±5	Base metal

sizes in the base metal and weld metal are 1.695 μm and 0.25 μm , respectively. Furthermore, a decrease in grain size of the weld metal, as compared to the base metal, and the decrease of size and distribution of carbides in the welding metal, as compared to the base metal, lead to an increase in hardness of the weld metal in comparison to the base metal. Solidification of the weld metal is dendritic. The dendrites in the central zone of the welding are fine and equiaxed while they are larger and columnar in the fusion line. Epitaxial growth was observed in the interface of base metal and weld metal. Alloy elements segregation did not occur during the solidification process and fine cracks were not observed in the welding zone of the alloy.

References

1. E. F. Bradley, "Welding of Superalloys, A Technical Guide", 1989, pp.197-90.
2. J. K. Tien, "Super Alloy, Super Composite and Super Ceramics", 1989, pp.1-14 & 142-144.
3. J. Wily, Inc. Sons, "The Super Alloys", 1976, pp.509-532.
4. D. F. Paulonis, W.A. Owczaski, "Joining of Powder Metal Superalloys", 1980, pp. 77-102.
5. M. Arkoosh, N. F.Fiore, "Elevated Temperature Ductility Minimum in Hastelloy X", Metallurgical Transactions, Vol. 3, Aug. 1972, 935.
6. M. Aghaie, N. Golarzi, "Dynamic and Metadynamic Recrystallization of Hastelloy X Superalloy", J Mater Sci, 43, 2008, pp. 3717–3724.
7. R.V. Miner, M.G. Castelli, "Hardening Mechanisms in a Dynamic Strain Aging Alloy, HastelloyX, during Isothermal and Thermomechanical Cyclic Deformation", Metallurgical Transactions A, Vol. 23A, Feb., 1992, 551.
8. H. M. Tawancy, "Long-Term Ageing Characteristics of Hastelloy X", J Mater Sci 18, 1983, pp. 2976-2986.
9. Li. Zhang, S. L. Gobbi, K. H. Richter, "Autogenous Welding of Hastelloy X to Mar-M 247 by Laser", J MaterPro Tech ,70, 1997, pp. 285-292.
- 10.S. Muraoka, H. Itami, S. Nomura, "Carburization of Hastelloy X", J Nuclear Mater, 1975, 58 , pp. 18-24.
- 11.J. Matthew, S. Donachie, J. Donachie, "Superalloys, A Technical Guide", 2nd ed., ASM International, USA, New York, 2002, pp. 192-265.
- 12.J. C. Lippold, J. W. Sowards, G. M. Murray, B. T. Alexandrov, A. J. Ramirez, "Weld Solidification Cracking in Solid-Solution Strengthened Ni-Base Filler Metals", 2008, pp. 147-170.
- 13.M. Pang, G. Yu, H. H. Wang, C. Y. Zheng, "Microstructure Study of Laser Welding Cast Nickel-Based Super Alloy K418", J Mater Pro Tech, 207, 2008, pp. 271–275.
- 14.G. D. Janaki Ram, A. Venugopal Reddy, K. Prasad Rao, G. M. Reddy, J. K. Sarin Sundar, "Microstructure and Tensile Properties of Inconel 718 Pulsed Nd-YAG Laser Welds", J Mater Pro Tech, 167, 2005, pp. 73–82.
- 15.M. Shamanian, A. Ashrafi, "Welding of Metallurgy", Isfahan University of Technology, 1388.
- 16.N. S. Stoloff, "Speciality Steels and Heat-Resistant Alloy", Metals Handbook, 1st ed., Vol. 1, ASM Handbook, 2005, pp. 1478-1549.